

## Supporting Information

for

### **Arene ruthenium(II) complexes induce S-phase arrest in MG-63 cells through stabilization of *c-myc* G-quadruplex DNA**

**Cundong Fan,<sup>#,a]</sup> Qiong Wu,<sup>#,b]</sup> Tianfeng Chen,<sup>\*[a]</sup> Yibo Zhang,<sup>[a]</sup> Wenjie Zheng,<sup>\*[a]</sup> Qi Wang,<sup>[b]</sup> and Wenjie Mei<sup>\*[b]</sup>**

<sup>a</sup>*Department of Chemistry, Jinan University, Guangzhou, 510632, China*

<sup>b</sup>*School of Pharmacy, Guangdong Pharmaceutical University, Guangzhou, 510006, China*

## **EXPERIMENTAL SECTION**

### **1. Materials and chemicals**

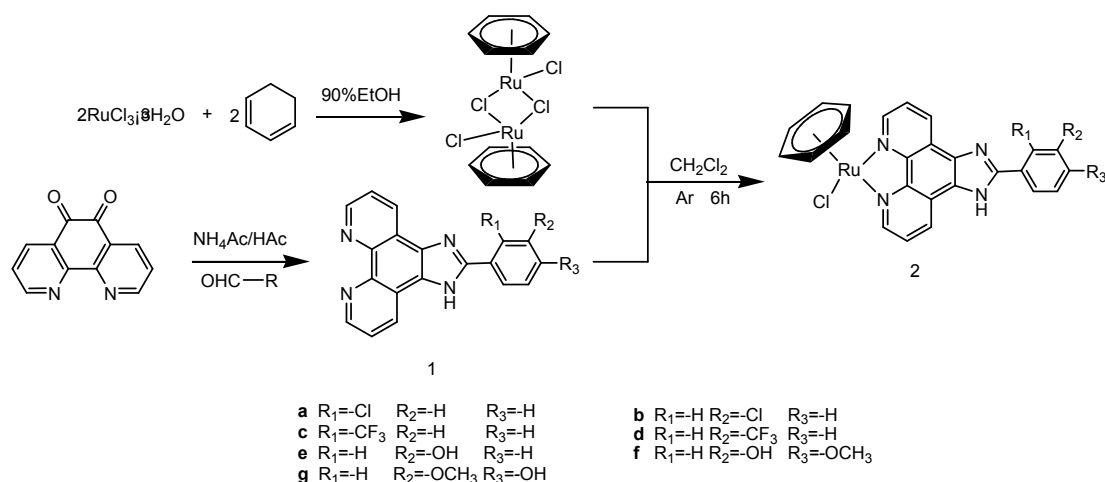
All used chemicals were obtained from commercial vendors and used as received. Ru(III) chloride hydrate was purchased from Mitsuwa Chemicals. 1,10-Phenanthroline monohydrate, 1,3-cyclohexadiene and benzaldehydes and its derivative were obtained from Aladdin. *c-myc* oncogene DNA (oligonucleotide sequences: 5'-TGGGGAGGGTGGGGAGGGTGGGGAAGG-3') was purchased from Sangon Biotechnology Company and formed G-quadruplexes conformation when 4 °C renaturation for 24 h after 90 °C denaturation for 5 min as literature described.<sup>1</sup> Propidium iodide (PI), 3-[4,5-dimethyl-thiazol-2-yl]-2,5 -diphenyltetrazolium bromide (MTT) and bicinchoninic acid (BCA) kit for protein determination were purchased from Sigma. Reagent kit for single cell gel electrophoresis assay (Comet Assay) was purchased from Trevigen. Dulbecco's modified Eagle's medium (DMEM), fetal bovine serum (FBS) and the antibiotic mixture (penicillin-streptomycin) were purchased from Invitrogen (Carlsbad, CA). All of the antibodies used in this study were purchased from Cell Signaling Technology (Beverly, MA). All of the solvents used were of high-performance liquid chromatography (HPLC) grade. The water used for all experiments was supplied by a Milli-Q water purification system (Millipore). The Tris-HCl buffer consisting of Tris (10 mM) and KCl (100 mM) was adjusted pH to 7.4 by HCl (0.1 mol), which was applied to UV titration, fluorescence quenching, CD spectrum and CD melting.

### **2. Physical measurements**

For the X-ray Crystallography, all reflection intensities were measured at 293(2) K on a Bruker SMART APEX 2K CCD-based X-ray diffractometer equipped. The collected frames were processed with the software SHELXTL with 2001 Bruker Analytical X-ray Solutions. NMR spectra were recorded in DMSO-*d*<sub>6</sub> on BrukerDRX2500 spectrometer. ESI-MS spectra were obtained in methanol on Agilent 1100 ESI-MS system operating at room temperature. The electronic emission spectra

were recorded on a Shimadzu UV-2550 Spectrophotometer and the steady-state fluorescence emission spectra were recorded on a RF-5301 Fluorescence Spectrophotometer. CD spectra were recorded on Jasco J810 Circular Dichroism (CD) Spectrophotometer. The stained cells were analyzed with Epics XL-MCL flow cytometer (Beckman Coulter, Miami, FL). Western blot analysis experiments were visualized on X-ray film using an enhanced chemiluminescence system (Kodak). Comet assay experiments were immediately pipetted onto the slide (CometSlide™) and used an image analysis system (Komet 3.1, Kinetics Imaging Ltd., Liverpool) linked to a CCD camera.

### 3. Synthesis and Characterization



Scheme S1. The Synthetic route of arene Ru(II) complexes.

**Synthesis of *o*-CIPIP (1a):** The ligand 2-(2-chlorophenyl)-1*H*-imidazo[4,5*f*][1,10]phenanthroline (*o*-CIPIP) was prepared by using the similar method as the literatures with some modifications and were used after further purification.<sup>2</sup> 10-phenanthroline-5,6-dione (1.6 mmol, 347 mg) and 2-chlorobenzaldehyde (1.6 mmol, 224 mg) in 20 ml HAc and 2.53 g  $\text{NH}_4\text{Ac}$  solution was refluxed at 110°C for 4 h. Then 20 ml of water was added and pH value was adjusted to 7.0 at room temperature. Filter, and dry in vacuum to obtain a yellow precipitate. The product was purified in a silica gel column by using ethanol as eluent. Yield 348 mg, 65.9%.

**Synthesis of *m*-ClPIP (1b):** The ligand 2-(3-chloro-phenyl)-1*H*-imidazo-[4,5*f*][1,10]phenanthroline (*m*-ClPIP) was prepared from 1,10-phenanthroline-5,6-dione (1.6 mmol, 347 mg) and 3-(chlorophenyl)benzaldehyde (1.6 mmol, 224 mg) using the similar method. Yield 362 mg, 68.6%.

**Synthesis of *o*-TFPIP (1c):** The ligand 2-(2-(trifluoro-methyl)phenyl)-1*H*-imidazo-[4,5*f*][1,10]phenanthroline (*o*-TFPIP) was prepared from 1,10-phenanthroline-5,6-dione (1.6 mmol, 347 mg) and 2-(trifluoromethyl) benzaldehyde (1.6 mmol, 278.4 mg) using the similar method. Yield 378 mg, 64.9%.

**Synthesis of *m*-TFPIP (1d):** The ligand 2-(3-(trifluoro-methyl)phenyl)-1*H*-imidazo-[4,5*f*][1,10]phenanthroline (*m*-TFPIP) was prepared from 1,10-phenanthroline-5,6-dione (1.6 mmol, 347 mg) and 3-(trifluoromethyl)benzaldehyde (1.6 mmol, 278.4 mg) using the similar method. Yield 358 mg, 61.5%.

**Synthesis of *m*-HPIP (1e):** The ligand 2-(3-(hydroxyl-phenyl)-1*H*-imidazo-[4,5*f*][1,10]phenanthroline (*m*-HPIP) was prepared from 1,10-phenanthroline-5,6-dione (1.6 mmol, 347 mg) and formaldehyde (1.6 mmol, 195.2 mg) using the similar method. Yield 325 mg, 65.1%.

**Synthesis of *m*-OH-*p*-OMePIP (1f):** The ligand 2-(3-hydroxy-4-methoxyphenyl)-1*H*-imidazo-[4,5*f*][1,10]phenanthroline (*m*-OH-*p*-OMePIP) was prepared from 1,10-phenanthroline-5,6-dione (1.6 mmol, 347 mg) and 3-hydroxy-4-methoxybenzaldehyde (1.6 mmol, 243.2 mg) using the similar method. Yield 341 mg, 62.3%.

**Synthesis of *m*-OM-*p*-OHPIP (1g):** The ligand 2-(2-hydroxy-4-methoxyphenyl)-1*H*-imidazo-[4,5*f*][1,10]phenanthroline (*m*-OMe-*p*-OHPIP) was prepared from 1,10-phenanthroline-5,6-dione (1.6 mmol, 347 mg) and 2-hydroxy-4-methoxybenzaldehyde (1.6 mmol, 243.2 mg) using the similar method. Yield 329 mg, 60.1%.

**Synthesis of [(C<sub>6</sub>H<sub>6</sub>)Ru(*o*-ClPIP)Cl]Cl (2a):** A mixture of [(C<sub>6</sub>H<sub>6</sub>)RuCl<sub>2</sub>]<sub>2</sub> (0.15 mmol, 75 mg) and *o*-ClPIP (0.3 mmol, 99.3 mg) in dichlormethane (40 mL) was

refluxed under argon for 6 h until the solution color changed from brown to yellow.<sup>3</sup> A yellow precipitate was obtained by rotary evaporator and purified by recrystallization in distilled water. Yield 105 mg, 56.7%. Anal. Calcd. for  $C_{29}H_{39}Cl_2N_4O_6Ru$  ( $[(C_6H_6)Ru(o\text{-ClPIP})Cl]Cl \cdot 2MeOH \cdot 4H_2O$ ): C, 48.95; H, 5.52; N, 7.87. Found: C, 49.03; H, 5.46; N, 7.79. ESI-MS (in MeOH):  $m/z$  546.1, ( $[M-Cl]^+$ ).  $^1H$  NMR (DMSO- $d_6$ ,  $\delta$  ppm)  $\delta$ : 9.98 (dd,  $J = 5.3, 1.2$  Hz, 2H), 9.25 (d,  $J = 8.0$  Hz, 2H), 8.21 (dd,  $J = 8.2, 5.3$  Hz, 2H), 7.9 (m, 1H), 7.75 (m, 1H), 7.62 (m, 2H), 6.33 (s, 6H).  $^{13}C$  NMR (DMSO- $d_6$ ,  $\delta$  ppm)  $\delta$ : 154.67 (s), 150.99 (s), 143.90 (s), 133.13 (s), 132.72 (s), 132.52 (s), 132.15 (s), 130.93 (s), 129.68 (s), 127.98 (s), 126.63 (s), 87.32 (d,  $J = 16.5$  Hz), 40.49 (s), 40.27 (d,  $J = 13.8$  Hz), 40.16 (s), 39.99 (s), 39.83 (s), 39.66 (s), 39.49 (s).

**Synthesis of  $[(C_6H_6)Ru(m\text{-ClPIP})Cl]Cl$  (2b):** 2b was prepared in a similar method to that of above, but with *m*-ClPIP (0.3 mmol, 99.3 mg) in place of *o*-ClPIP. Yield 98 mg, 52.9%. Anal. Calcd. for  $C_{28}H_{33}Cl_2N_4O_4Ru$  ( $[(C_6H_6)Ru(m\text{-ClPIP})Cl]Cl \cdot MeOH \cdot 3H_2O$ ): C, 50.83; H, 5.03; N, 8.47. Found: C, 50.91; H, 4.98; N, 8.35. ESI-MS (in MeOH):  $m/z$  546.1, ( $[M-Cl]^+$ ).  $^1H$  NMR (DMSO- $d_6$ ,  $\delta$  ppm)  $\delta$ : 9.96 (dd,  $J = 5.3, 1.1$  Hz, 2H), 9.35 (s, 2H), 8.43 (d,  $J = 11.5$  Hz, 1H), 8.38 (dd,  $J = 10.3, 5.3$  Hz, 1H), 8.20 (dd,  $J = 8.1, 5.4$  Hz, 2H), 7.62 (m, 2H), 6.33 (s, 6H).  $^{13}C$  NMR (DMSO- $d_6$ ,  $\delta$  ppm)  $\delta$ : 144.45 (s), 141.02 (s), 135.90 (s), 134.00 (s), 133.05 (s), 132.40 (s), 131.74 – 130.21 (m), 128.80 (s), 127.65 – 123.48 (m), 87.14 (s), 40.62 (s), 40.07 (s), 39.97 (s), 39.74 (s), 39.56 (s), 39.46 (s).

**Synthesis of  $[(C_6H_6)Ru(o\text{-TFPIP})Cl]Cl$  (2c):** 2c was prepared in a similar method to that of above, but with *o*-TFPIP (0.3 mmol, 109.5 mg) in place of *o*-ClPIP. Yield: 115 mg, 58.9%. Anal. Calcd. for  $C_{30}H_{35}ClF_3N_4O_4Ru$  ( $[(C_6H_6)Ru(o\text{-TFPIP})Cl]Cl \cdot 2MeOH \cdot 2H_2O$ ): C, 50.81; H, 4.97; N, 7.90. Found: C, 50.73; H, 4.88; N, 7.93. ESI-MS (in MeOH):  $m/z$  579.13, ( $[M-Cl]^+$ ).  $^1H$  NMR (DMSO- $d_6$ ,  $\delta$  ppm)  $\delta$ : 9.96 (dd,  $J = 5.3, 1.1$  Hz, 2H), 9.06 (dd,  $J = 62.6, 8.1$  Hz, 2H), 8.16 (m, 2H), 8.02 (t,  $J = 11.0$  Hz, 2H), 7.86 (m, 2H), 6.32 (s, 6H).  $^{13}C$  NMR (DMSO- $d_6$ ,  $\delta$  ppm)  $\delta$ : 154.19 (s), 150.14 (s), 147.23 (s), 143.99 (s), 141.59 (s), 126.26 (s), 126.26 (s), 123.83 (s),

122.25 (s), 119.08 (s), 114.37 (s), 112.58 (s), 87.22 (s), 77.23 (s), 74.06 (s), 71.87 (m), 65.47 (s), 61.40 (s), 59.21 (s), 56.18 (s), 49.05 (s), 40.63 (s), 40.04 (s), 39.92 (s), 39.81 (s), 39.64 (s), 39.47 (s).

**Synthesis of [(C<sub>6</sub>H<sub>6</sub>)Ru(*m*-TFPIP)Cl]Cl (2d):** 2d was prepared in a similar method to that of above, but with *m*-TFPIP (0.3 mmol, 109.5 mg) in place of *o*-ClPIP. Yield: 98 mg, 50.2%. Anal. Calcd. for C<sub>29</sub>H<sub>37</sub>ClF<sub>3</sub>N<sub>4</sub>O<sub>6</sub>Ru [(C<sub>6</sub>H<sub>6</sub>)Ru(*m*-TFPIP)Cl]Cl•MeOH•5H<sub>2</sub>O): C, 47.64; H, 5.10; N, 7.66. Found: C, 47.71; H, 5.17; N, 7.74. ESI-MS (in MeOH): *m/z* 579.13, ([M-Cl]<sup>+</sup>). <sup>1</sup>H NMR (DMSO-*d*<sub>6</sub>, δ ppm) δ: 9.97 (dd, *J* = 5.3, 1.1 Hz, 2H), 9.33 (s, 2H), 8.67 (dd, *J* = 24.1, 7.8 Hz, 2H), 8.22 (m, 2H), 7.90 (dt, *J* = 15.2, 7.7 Hz, 2H), 6.33 (s, 6H).

**Synthesis of [(C<sub>6</sub>H<sub>6</sub>)Ru(*m*-HPIP)Cl]Cl (2e):** 2e was prepared in a similar method as described above, but with *m*-HPIP (0.3 mmol, 93.9 mg) in place of *o*-ClPIP. Yield: 102 mg, 56.8%. Anal. Calcd. for C<sub>30</sub>H<sub>46</sub>ClN<sub>4</sub>O<sub>9</sub>Ru [(C<sub>6</sub>H<sub>6</sub>)Ru(*m*-HPIP)Cl]Cl•2MeOH•6H<sub>2</sub>O): C, 48.48; H, 6.24; Cl, 4.77; N, 7.54. Found: C, 48.61; H, 6.31; N, 4.69. ESI-MS (in MeOH): *m/z* 527.01, ([M-Cl]<sup>+</sup>). <sup>1</sup>H NMR (DMSO-*d*<sub>6</sub>, δ ppm) δ: 9.89 (m, 2H), 9.85 (s, 2H), 9.34 (s, 2H), 8.19 (dd, *J* = 8.0, 5.4 Hz, 1H), 7.92 – 7.72 (m, 1H), 7.41 (dd, *J* = 17.9, 10.0 Hz, 1H), 6.98 (dd, *J* = 7.9, 2.0 Hz, 1H), 6.33 (s, 6H).

**Synthesis of [(C<sub>6</sub>H<sub>6</sub>)Ru(*m*-OH-*p*-OMPIP)Cl]Cl (2f):** 2f was prepared in a similar method to that of above, but with *m*-OH-*p*-OMPIP (0.3 mmol, 103.2 mg) in place of *o*-ClPIP. Yield: 103 mg, 54.5%. Anal. Calcd. for C<sub>30</sub>H<sub>44</sub>ClN<sub>4</sub>O<sub>9</sub>Ru [(C<sub>6</sub>H<sub>6</sub>)Ru(*m*-OH-*p*-MOPIP)Cl]Cl•2MeOH•5H<sub>2</sub>O): C, 48.61; H, 5.98; N, 7.56. Found: C, 48.57; H, 6.03; N, 7.48. ESI-MS (in MeOH): *m/z* 559.09, ([M-Cl]<sup>+</sup>). <sup>1</sup>H NMR (DMSO-*d*<sub>6</sub>, δ/ppm) δ: 9.92 (d, *J* = 5.2 Hz, 2H), 9.40 (s, 2H), 9.18 (s, 2H), 8.17 (s, 2H), 7.79 (d, *J* = 7.6 Hz, 2H), 7.15 (d, *J* = 8.5 Hz, 2H), 6.30 (s, 6H).

**Synthesis of [(C<sub>6</sub>H<sub>6</sub>)Ru(*m*-OM-*p*-OHPIP)Cl]Cl (2g):** 2g was prepared in a similar method to that of above, but with *m*-OM-*p*-OHPIP (0.3 mmol, 103.2 mg) in place of *o*-ClPIP. Yield 112.5 mg, 59.5%. Anal. Calcd. for C<sub>29</sub>H<sub>36</sub>ClN<sub>4</sub>O<sub>6</sub>Ru [(C<sub>6</sub>H<sub>6</sub>)Ru(*m*-MO-*p*-OHPIP)Cl]Cl•MeOH•3H<sub>2</sub>O): C, 51.74; H, 5.39; N, 8.32. Found: C, 51.69; H,

5.47; N, 8.41. ESI-MS (in MeOH):  $m/z$  559.09,  $([M-Cl]^+)$ .  $^1H$  NMR (in DMSO- $d_6$ ,  $\delta/ppm$ )  $\delta$ : 9.97 (m, 2H), 9.37 (t,  $J = 66.5$  Hz, 2H), 8.3 (m, 2H), 8.19 (m, 2H) 6.7 (m, 2H), 6.35 (s, 6H).

#### 4. Crystallography

The crystal suitable for X-ray diffraction was obtained by recrystallization in methanol solution by adding petroleum ether into the solution slowly, and then the solution was kept in dark for seven days at room temperature to give a yellow block shaped crystals. The X-ray intensity data for **2e** was collected at X-ray diffractometer equipped with a graphite-monochromated MoK $\alpha$  radiation ( $\lambda=0.71073$  Å) by using an  $\omega$  scan mode ( $0.99^\circ < \theta < 27.12^\circ$ ).

#### 5. Biological study

##### 5.1 Cell Lines and Cell Culture

Several human cancer cell lines, including melanoma A375, hepatocellular carcinoma HepG2, cervical carcinoma Hela-229, neuroblastoma Neuro-2a, breast cancer MCF-7, prostatic cancer LNCap, osteosarcoma MG-63 cells and human normal kidney cells HK-2 were purchased from American Type Culture Collection (ATCC, Manassas, VA). All cell lines were maintained in DMEM medium supplemented with fetal bovine serum (10%), penicillin (100 units/ml) and streptomycin (50 units/ml) at 37°C in CO<sub>2</sub> incubator (95% relative humidity, 5% CO<sub>2</sub>).

##### 5.2 MTT Assay

All complexes were dissolved in DMSO with stock solution at 10 mg/ml. Cell viability was determined by measuring the ability of cells to transform MTT to a purple formazan dye.<sup>4</sup> Cells were seeded in 96-well tissue culture plates ( $3 \times 10^3$  cells/well) for 24 h. The cells were then incubated with the tested compounds at different concentrations for 72 h. After incubation, 20  $\mu$ l/well of MTT solution (5 mg/ml phosphate buffered saline) was added and incubated for 5 h. The medium was aspirated and replaced with 150  $\mu$ l/well DMSO to dissolve the formazan salt. The absorbance intensity, which reflects the cell growth condition, was measured at 570

nm using a microplate spectrophotometer (Versamax).

### **5.3 Flow Cytometric Analysis**

The cell cycle distribution was analyzed by flow cytometry as previously reported.<sup>5</sup> Treated or untreated cells were trypsinized, washed with PBS and fixed with 75% ethanol overnight at -20 °C. The fixed cells were washed with PBS and stained with propidium iodide (PI) (1.21 mg/ml Tris, 700 U/ml RNase, 50.1 µg/ml PI, pH=8.0) for 30 min in darkness. The stained cells were analyzed by flow cytometer (Beckman Coulter, Miami, FL). Cell cycle distribution was analyzed using MultiCycle software (Phoenix Flow Systems, San Diego, CA). Apoptotic cells with hypodiploid DNA content were measured by quantifying the sub-G1 peak in the cell cycle pattern. For each experiment, 10,000 events per sample were recorded.

### **5.4 Western Blot Analysis**

Total cellular proteins were extracted by incubating cells in lysis buffer obtained from Cell Signaling Technology and protein concentrations were determined by BCA assay. SDS-PAGE was done in 10% tricine gels loading equal amount of proteins per lane. After electrophoresis, separated proteins were transferred to nitrocellulose membrane and blocked with 5% non-fat milk in TBST buffer for 1 h. After then, the membranes were incubated with primary antibodies at 1:1,000 dilutions in 5% non-fat milk overnight at 4 °C, and then secondary antibodies conjugated with horseradish peroxidase at 1:2,000 dilution for 1 h at room temperature. Protein bands were visualized on X-ray film using an enhanced chemiluminescence system (Kodak). To assess the presence of comparable amount of proteins in each lane, the membranes were stripped finally to detect the  $\beta$ -actin. The protein expression rate was quantified by Quantity One software.

### **5.5 Comet Assay**

Single-cell gel electrophoresis for detection of DNA damage was performed using the Comet assay reagent kit purchased from Trevigen according to the manufacturer's instructions. Briefly, cells after treatment were harvested by centrifugation at 1500 rpm (20 °C, 5 min) and resuspended at  $1 \times 10^5$  cells/ml in PBS. The cell suspension



was mixed with melted LM agarose at a ratio of 1:10 (v/v). An aliquot (75  $\mu$ l) of the mixture was immediately pipetted onto the slide (CometSlide™). After refrigeration for 30 min, the slide was immersed in prechilled lysis solution and left on ice for 60 min, followed by immersing in freshly prepared alkaline solution (300 mM NaOH, 1 mM EDTA, pH>13) for 60 min on ice in darkness. After DNA unwinding, the slide was subjected to alkaline solution for electrophoresis in a Savant ps 250 system set at 300 mA and 1 volt/cm for 30 min. After electrophoresis, the slide was rinsed with distilled H<sub>2</sub>O, fixed in 70% ethanol for 5 min and air-dried overnight. DNA was stained with SYBR GreenI (Trevigen) and visualized under a fluorescence microscope (Nikon, Eclipse E600).

## 6. Stabilization of *c-myc* G-quadruplexes DNA

The interaction between the complexes and *c-myc* G4-DNA was examined by spectroscopic analysis. UV absorption spectra of complex **2a** were recorded at 270 nm and 293 nm and the titration was terminated when the intensity of those two bands did not change significantly upon addition of *c-myc* G4-DNA. The trend of characteristic absorption peak of this complex indicates that the binding constants between the metal complexes with *c-myc* G4-DNA. The electronic titration experiment of the arene Ru(II) complex in Tris-HCl buffer was performed by using a fixed complex concentration to which increments of the DNA stock solution were added. The concentration of the complex **2a** in the solution was 20  $\mu$ M and different concentrations of *c-myc* G4-DNA were added. Complex-DNA solutions were allowed to incubate for 3 min before the absorption spectra were recorded. The intrinsic binding constant  $K_b$  of Ru(II) complex to DNA was calculated from Eq.<sup>6</sup>

$$(\epsilon_a - \epsilon_f) / (\epsilon_b - \epsilon_f) = [b - (b^2 - 2K^2 C_t [DNA] / S)]^{1/2} / 2KC_t \quad (1)$$

$$b = 1 + KC_t + K[DNA] / 2S \quad (2)$$

The competitive binding experiments with a well-established quenching assay based on the displacement of the intercalating drug EB from G4-DNA may give further information regarding the DNA binding properties of the complex to DNA.<sup>7</sup> If a complex could replace EB from DNA-bound EB, the fluorescence of the solution

would be greatly quenched due to the fact that the free EB molecules were ready to be quenched by the surrounding water molecules.<sup>8</sup> The EB-DNA system excited at 530 nm shows a strong fluorescence at 600 nm. According to the quenching curve we can draw a preliminary conclusion that the complex can competitively bind DNA with EB.

The CD spectrum of *c-myc* G4 DNA in the presence or absence of **2a** was also recorded. *c-myc* with G-quartet structure have a strong positive CD signal at 263 nm and a negative CD signal at 243 nm. Complex **2a** has no intrinsic CD signals, as they are achiral. Therefore, any CD signal above 300 nm can be attributed to the interaction of complex with DNA.<sup>9</sup>

Typical CD melting curves were obtained by following the change in ellipticity as a function of temperature at 263 nm. The solutions were heated at a rate of 0.1 °C/min using free strained quartz cuvettes with a path length of 0.1 or 1.0 cm, resulting in the collection of 2 data points/°C. Analysis of the CD melting curves was conducted using standard procedures.

## RESULTS.

### 1. ESI-MS spectra

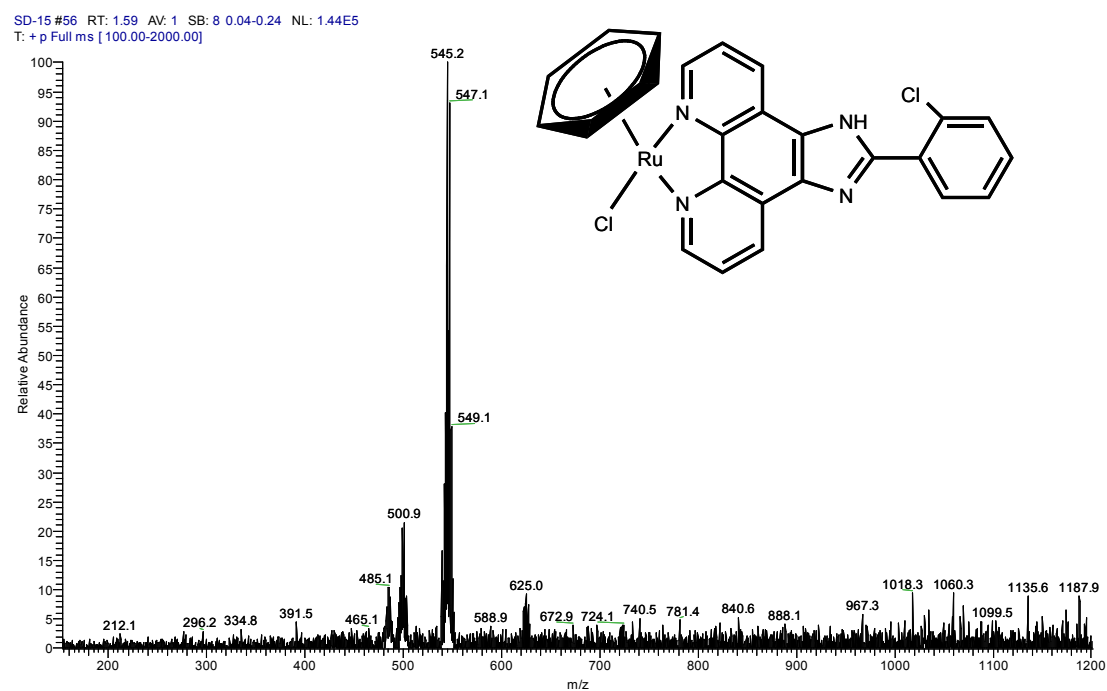


Figure S1. The ESI-MS spectra of complex **2a**

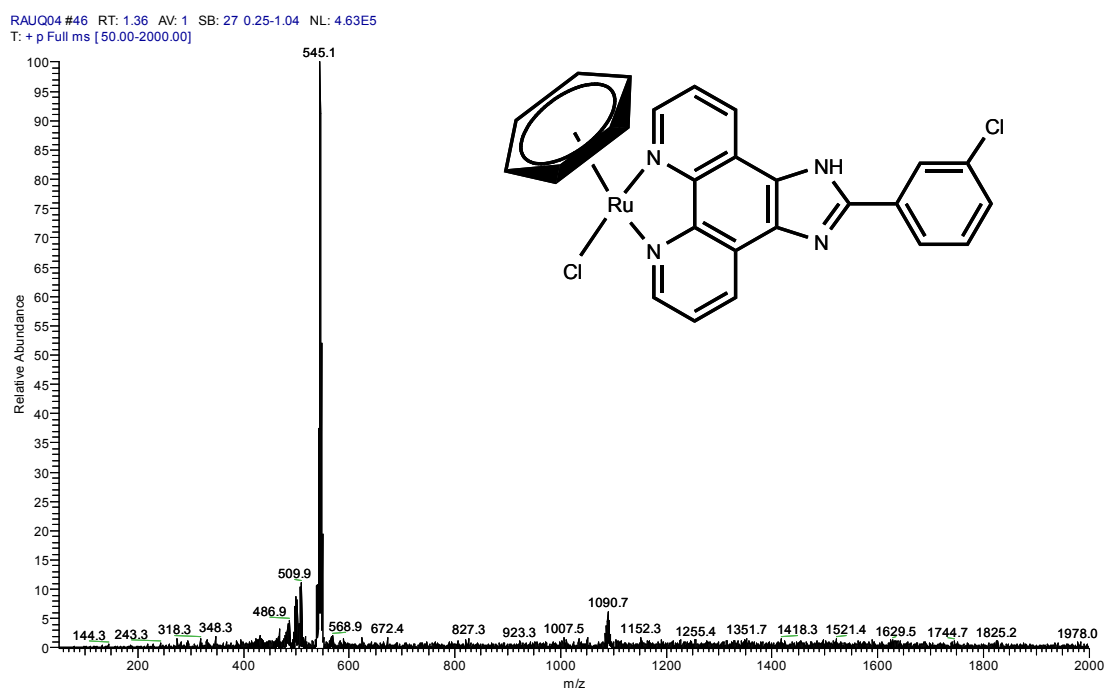


Figure S2. The ESI-MS spectra of complex **2b**

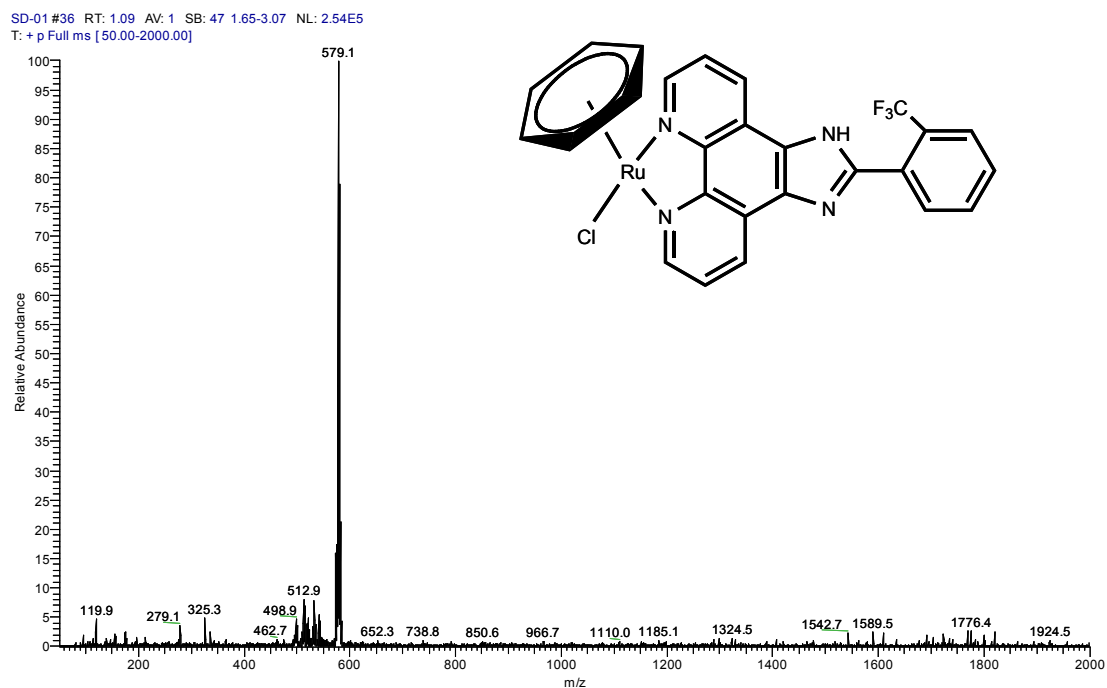


Figure S3. The ESI-MS spectra of complex **2c**

RAWQ05 #35-40 RT: 1.04-1.19 AV: 6 SB: 22 0.23-0.87 NL: 1.24E6  
T: + p Full ms [ 50.00-2000.00]

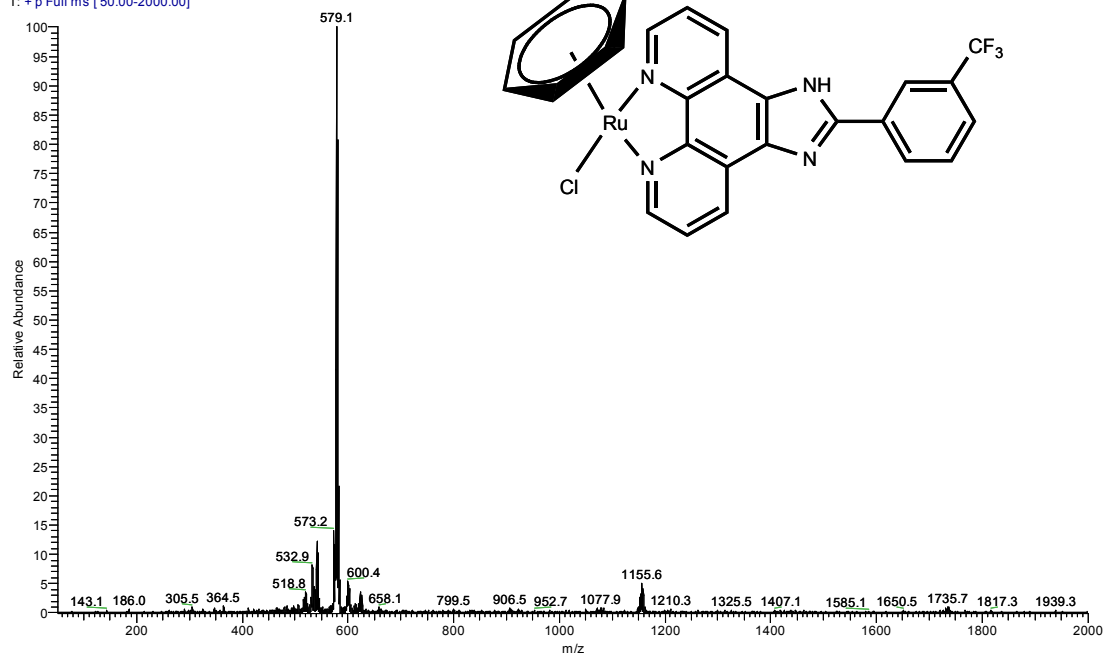


Figure S4. The ESI-MS spectra of complex 2d

SD-09 #21-22 RT: 0.61-0.64 AV: 2 SB: 6 0.28-0.43 NL: 1.72E6  
T: + p Full ms [ 100.00-2000.00]

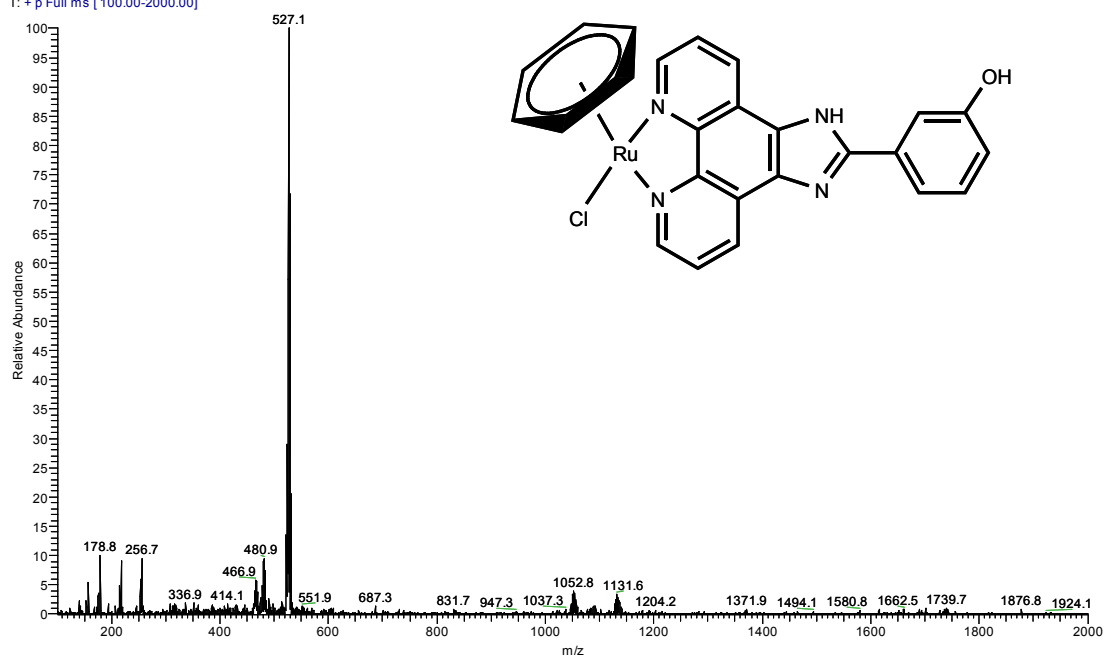


Figure S5. The ESI-MS spectra of complex 2e

sd-04 #32-38 RT: 0.98-1.16 AV: 7 SB: 7 0.62-0.80 NL: 4.38E5  
T: + p ms [50.00-2000.00]

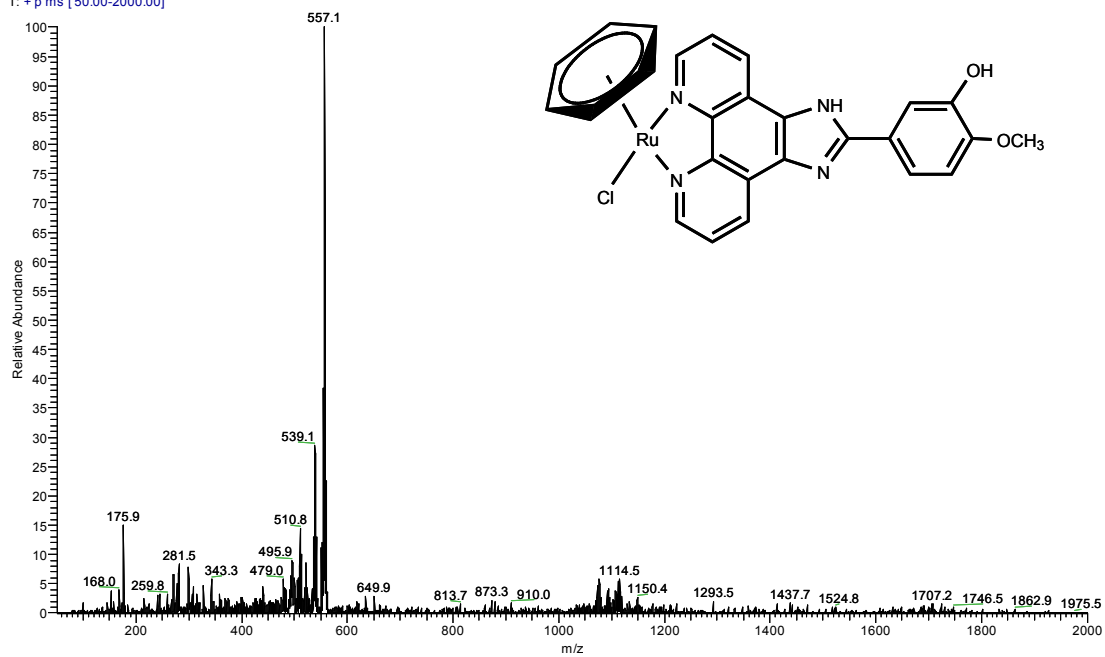


Figure S6. The ESI-MS spectra of complex **2f**

RAUQ01 #42 RT: 1.26 AV: 1 SB: 5 0.60-0.72 NL: 1.43E5  
T: + p ms [50.00-2000.00]

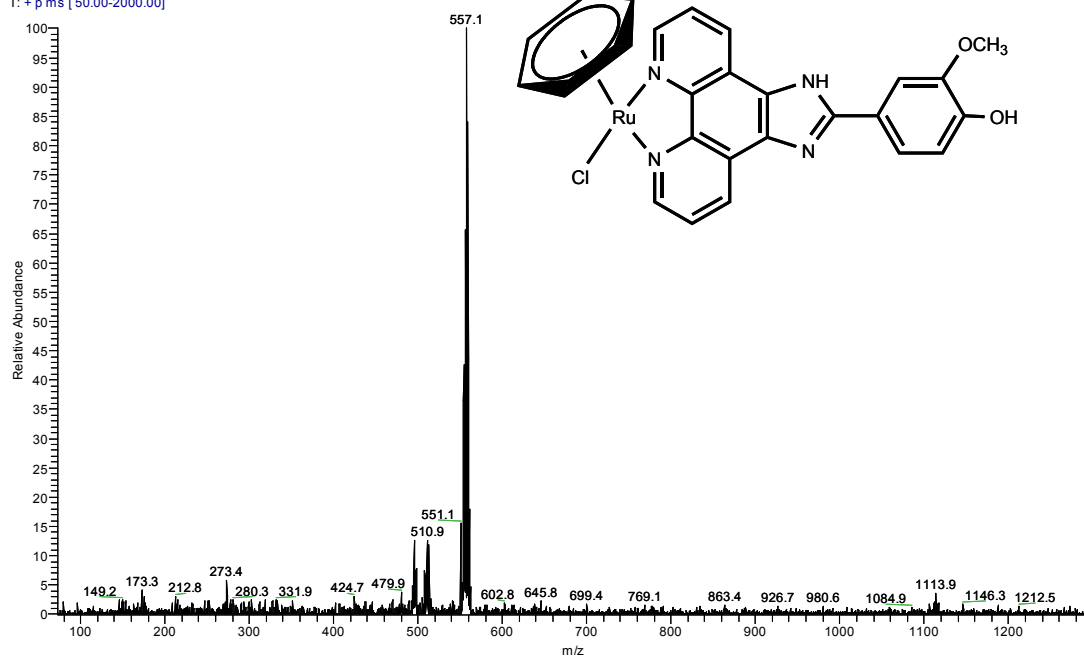


Figure S7. The ESI-MS spectra of complex **2g**

## 2. $^1\text{H}$ NMR spectra

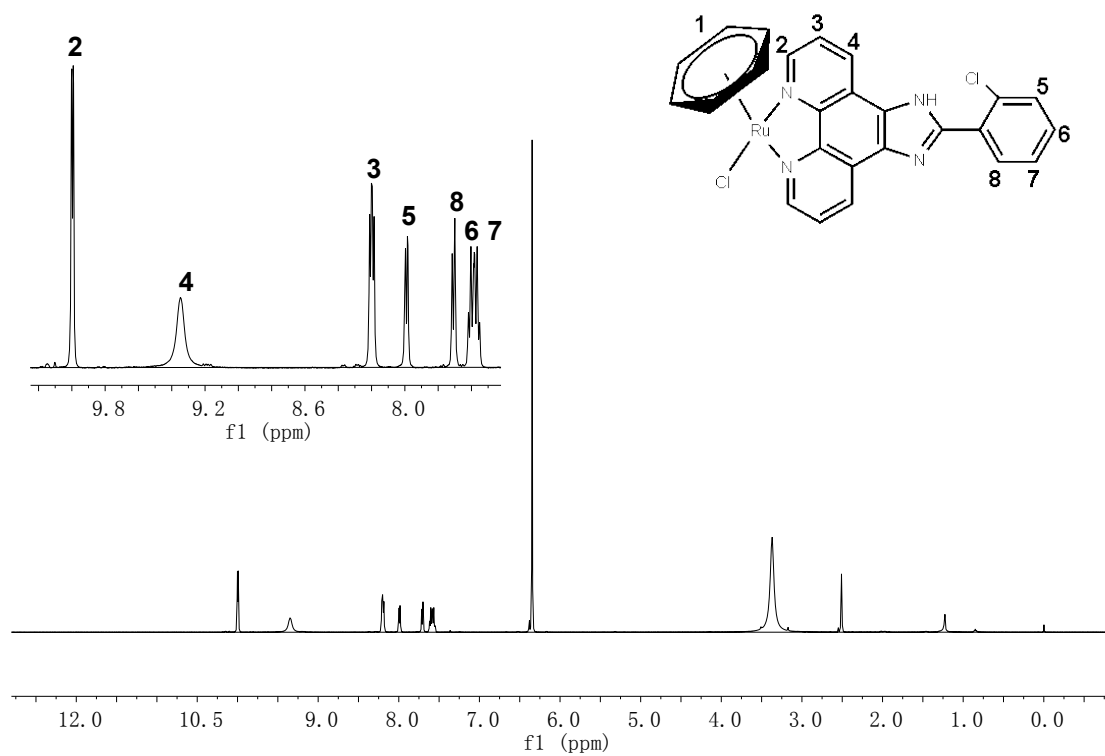


Figure S8. The  $^1\text{H}$  NMR spectra of complex **2a**

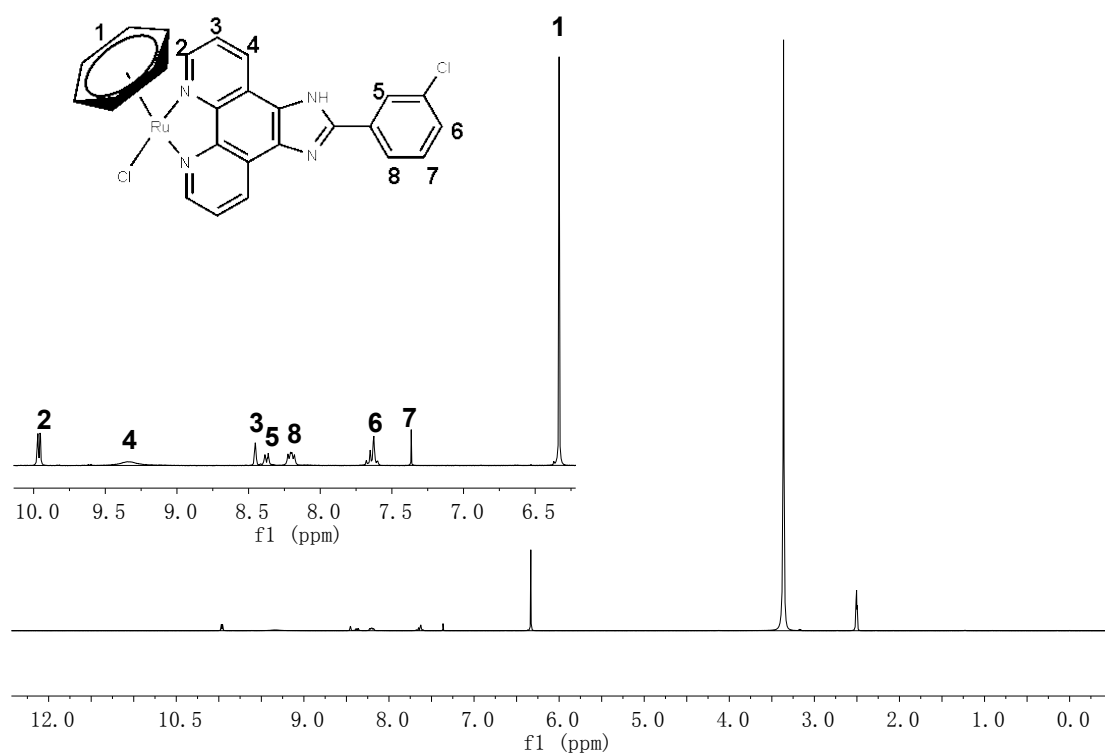


Figure S9. The  $^1\text{H}$  NMR spectra of complex **2b**

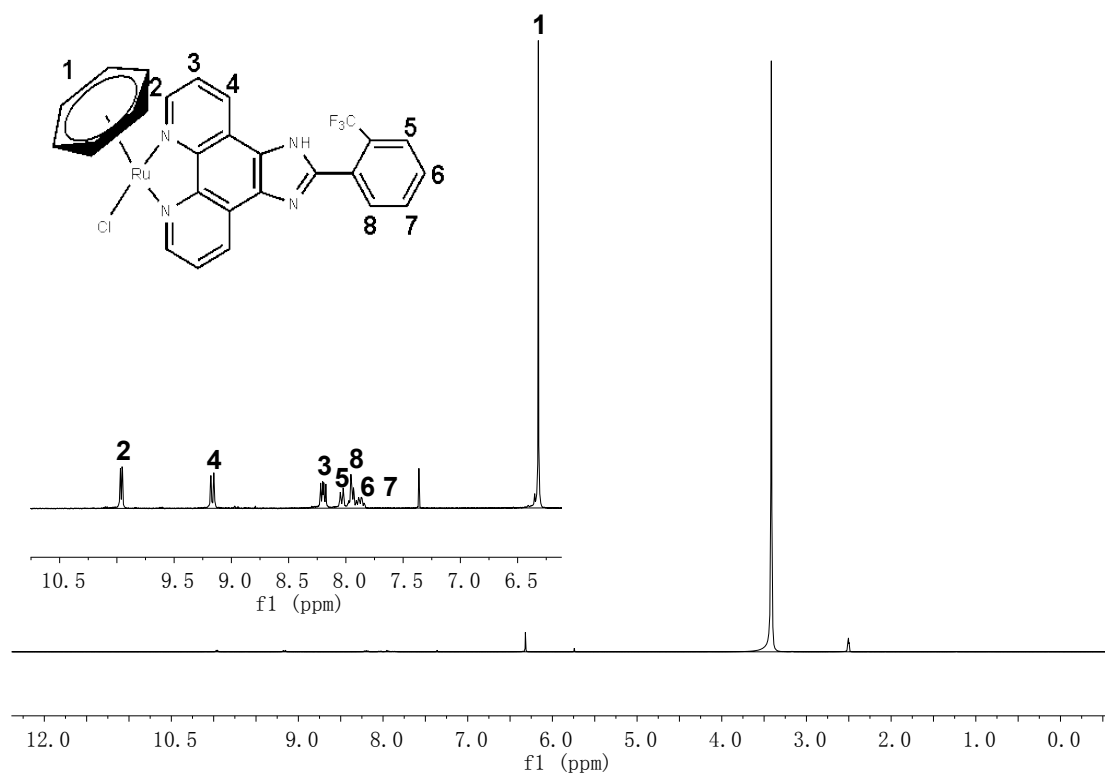


Figure S10. The  $^1\text{H}$  NMR spectra of complex **2c**

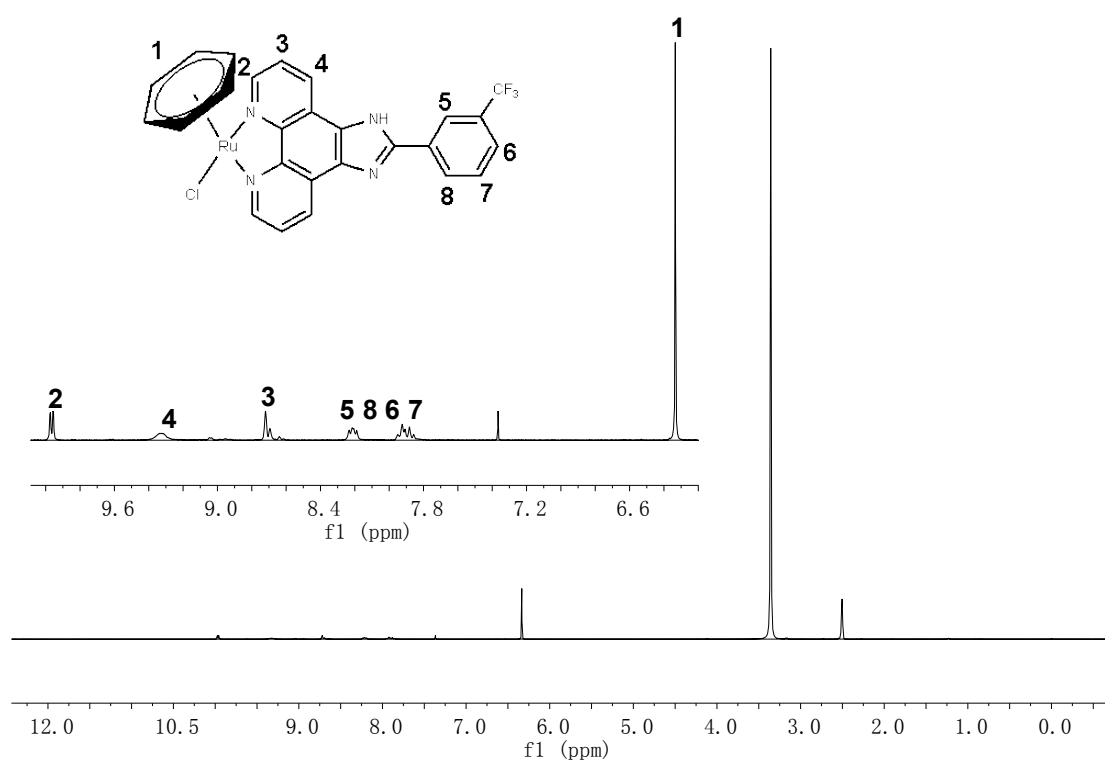


Figure S11. The  $^1\text{H}$  NMR spectra of complex **2d**

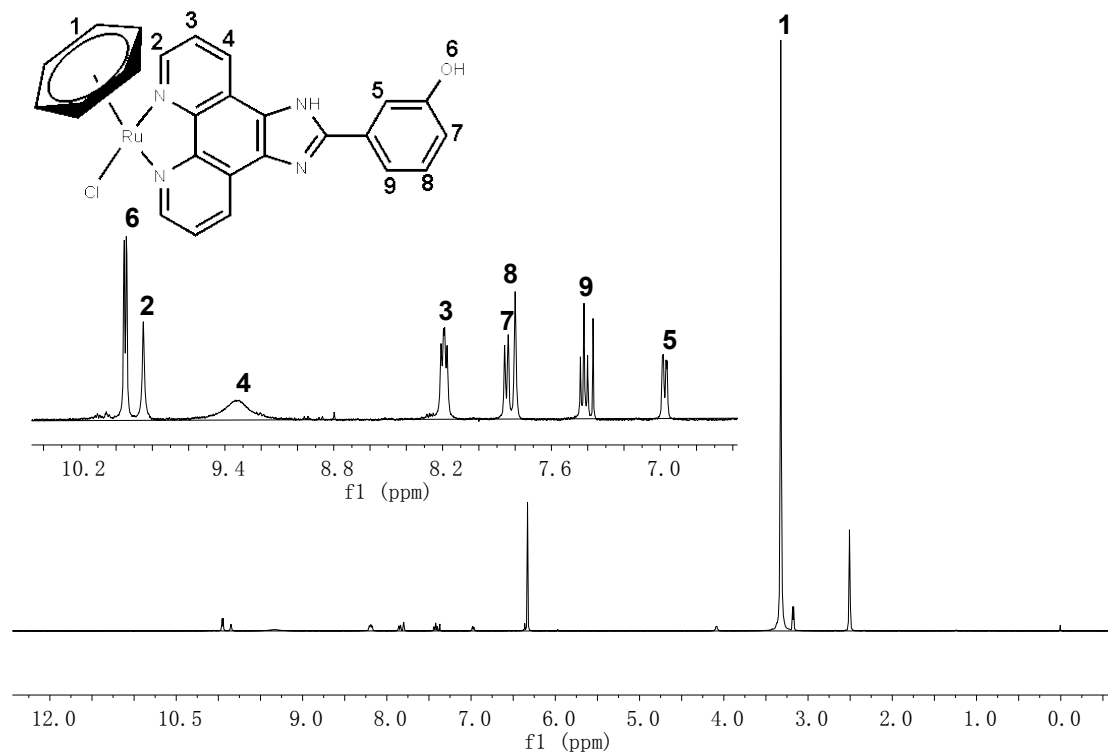


Figure S12. The  $^1\text{H}$  NMR spectra of complex **2e**

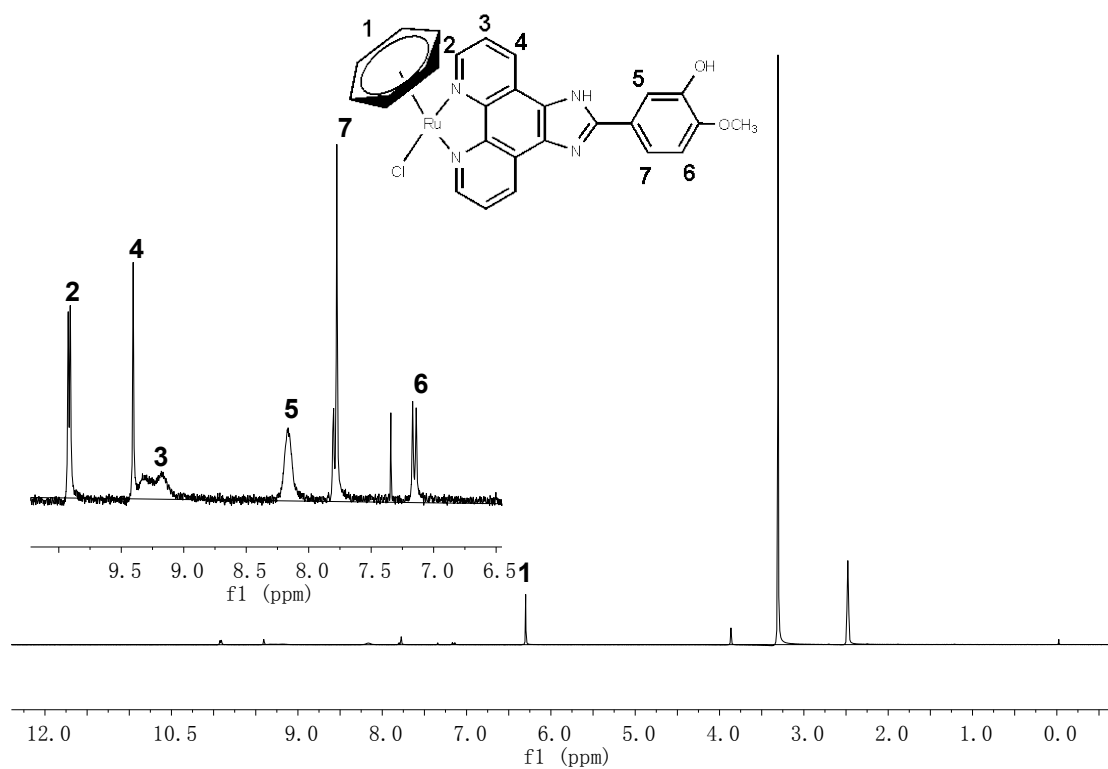
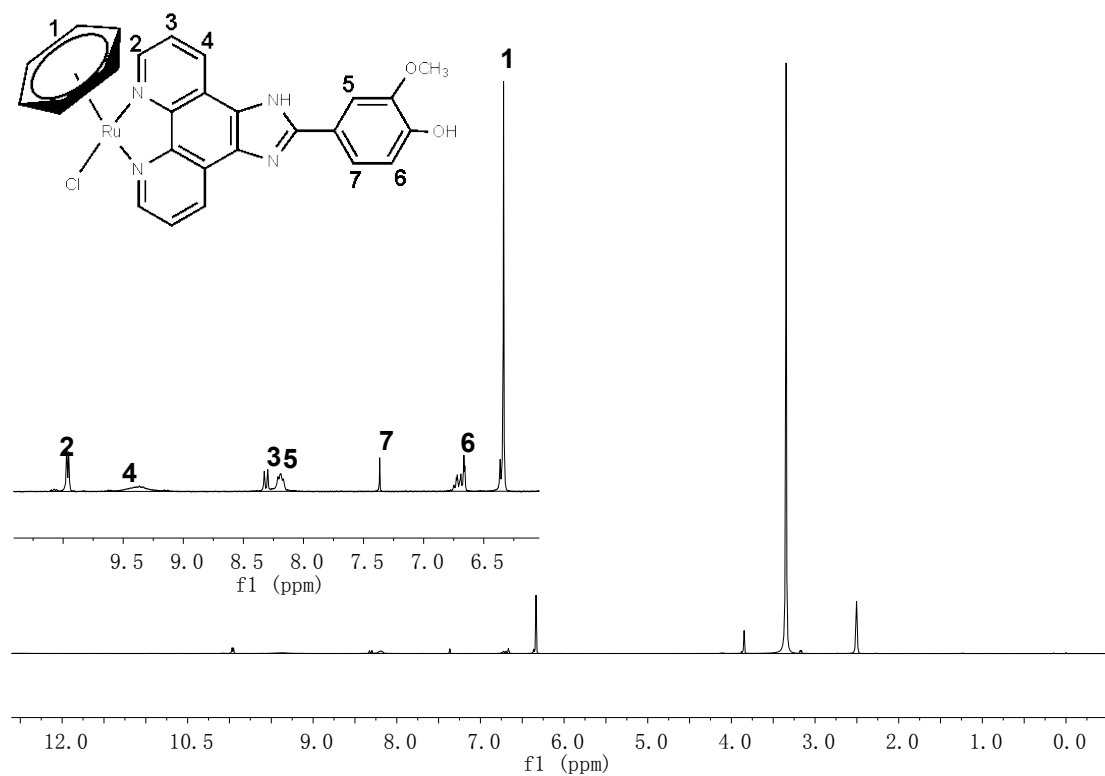
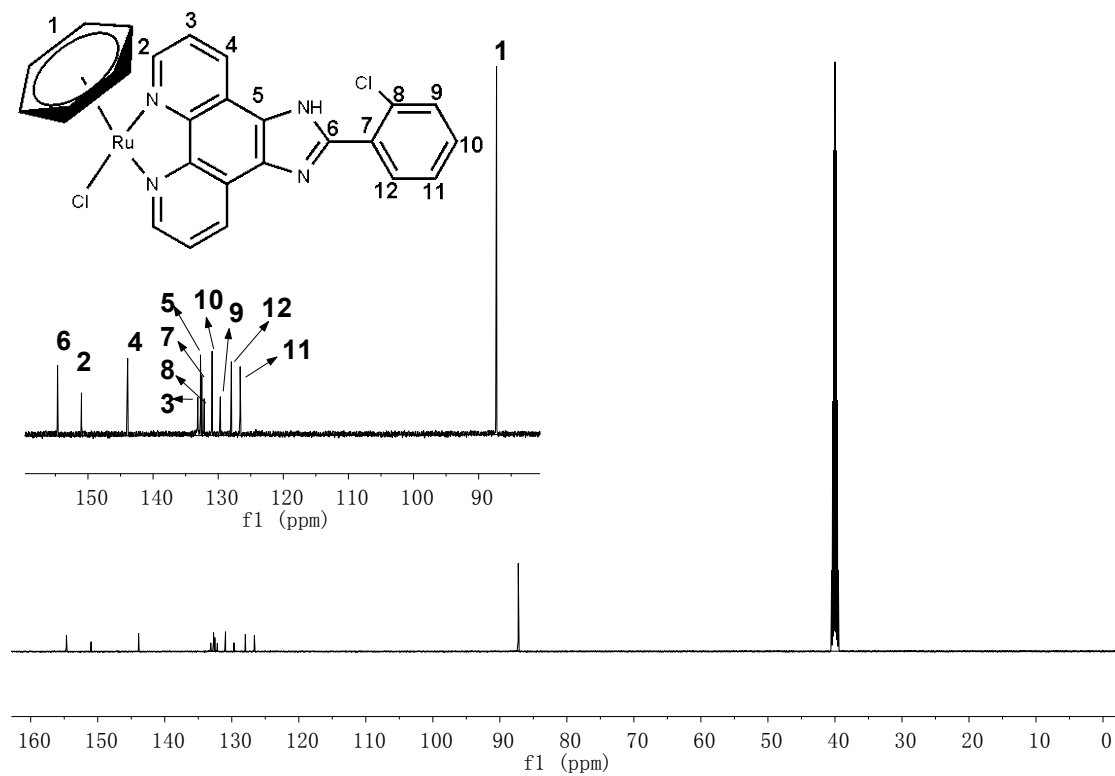


Figure S13. The  $^1\text{H}$  NMR spectra of complex **2f**





### 3. The $^{13}\text{C}$ NMR spectra



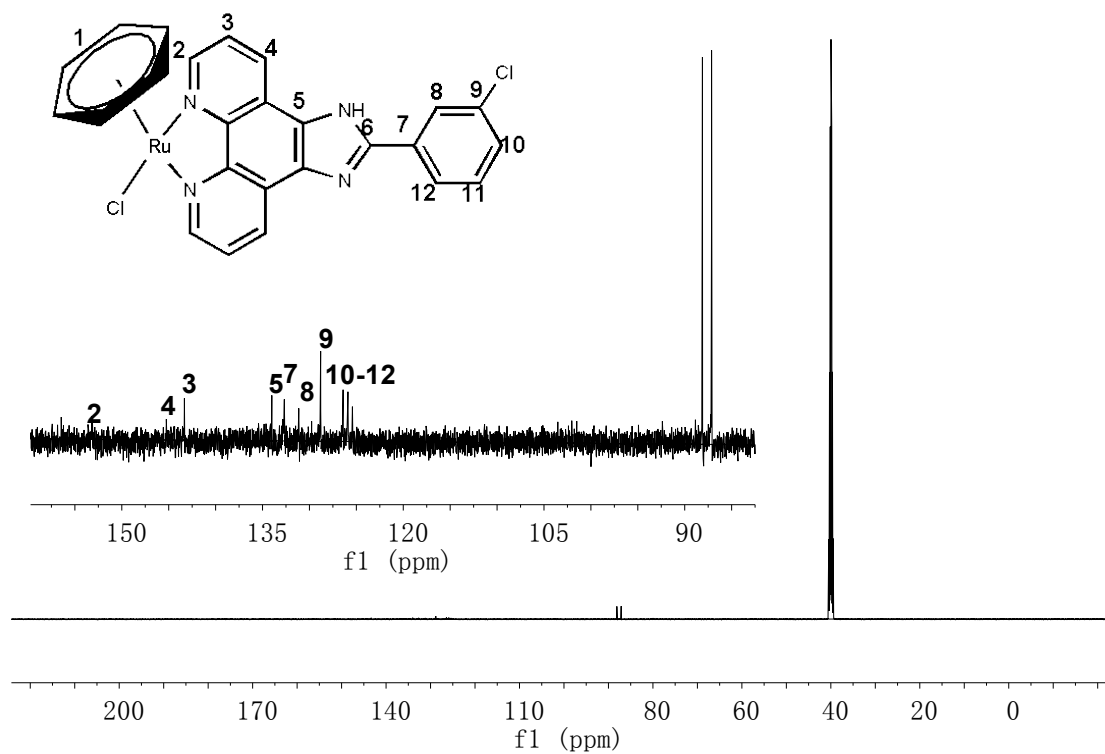


Figure S16. The  $^{13}\text{C}$  NMR spectra of complex **2b**

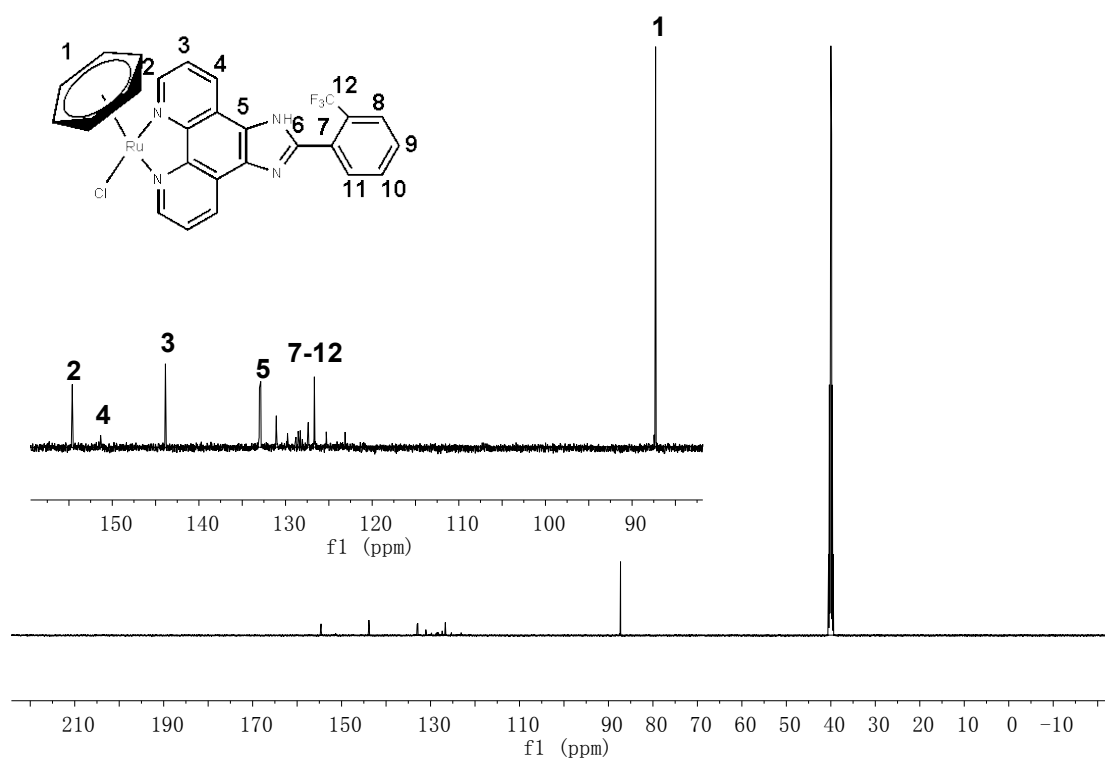


Figure S17. The  $^{13}\text{C}$  NMR spectra of complex **2c**

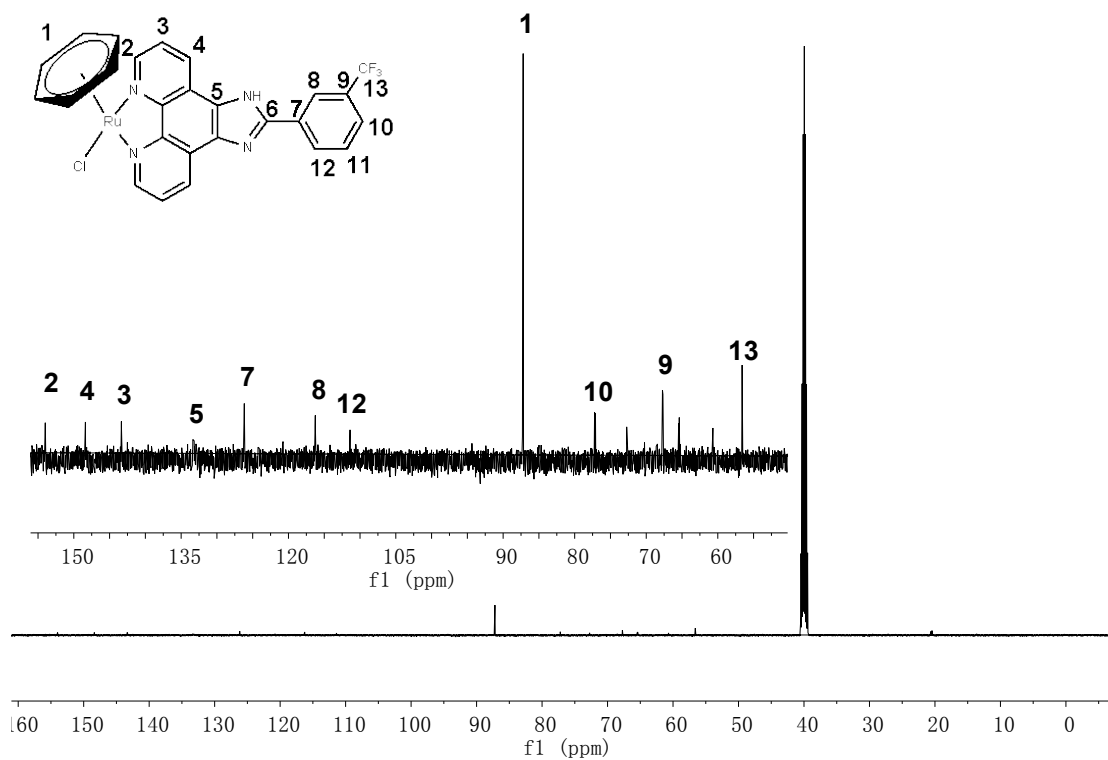


Figure S18. The  $^{13}\text{C}$  NMR spectra of complex **2d**

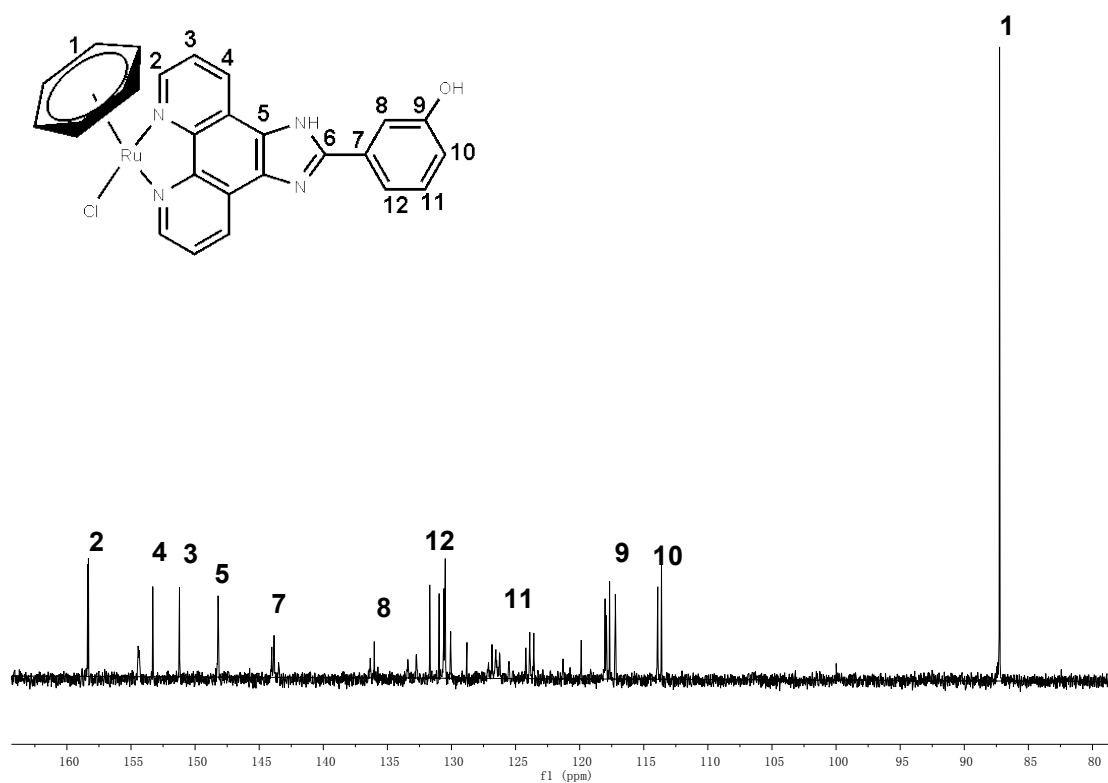


Figure S19. The  $^{13}\text{C}$  NMR spectra of complex **2e**

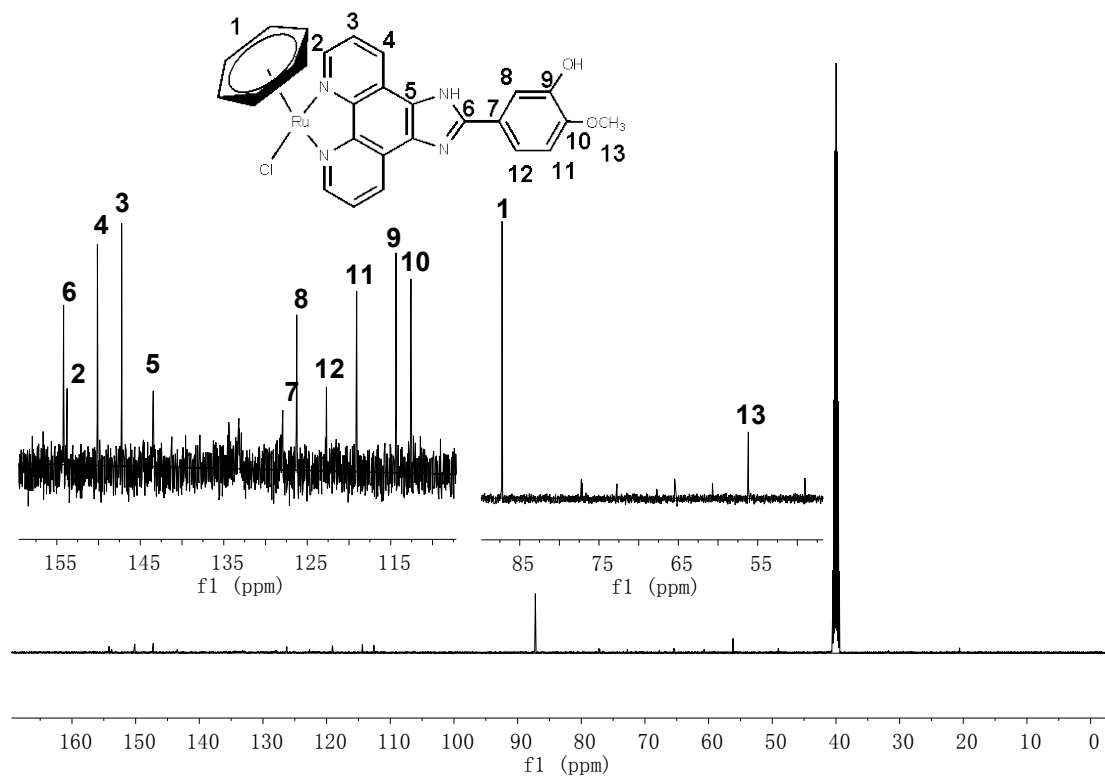


Figure S20. The  $^{13}\text{C}$  NMR spectra of complex **2f**

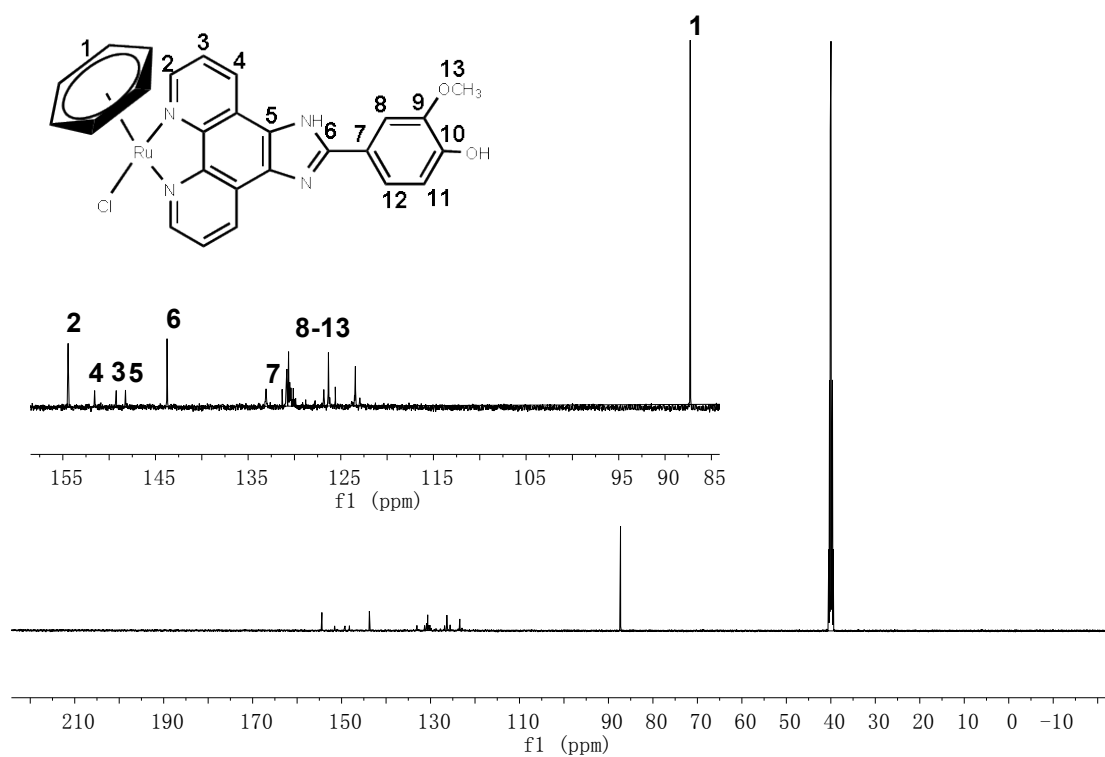


Figure S21. The  $^{13}\text{C}$  NMR spectra of complex **2g**

#### 4. HPLC Analysis

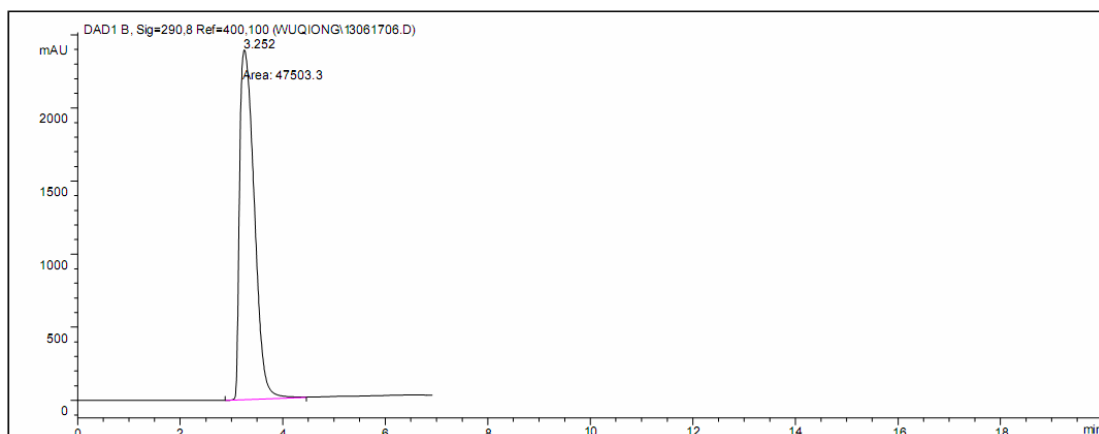


Figure S22. The HPLC analysis of complex **2a**

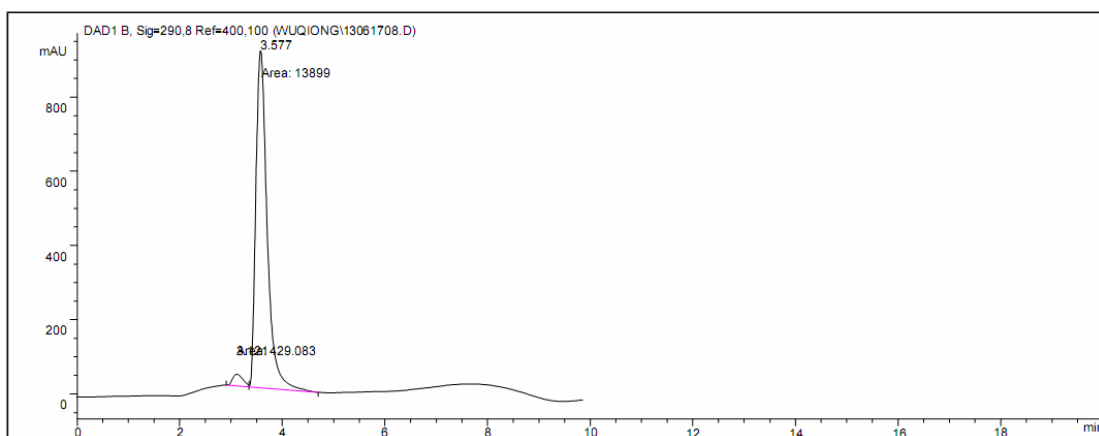


Figure S23. The HPLC analysis of complex **2b**

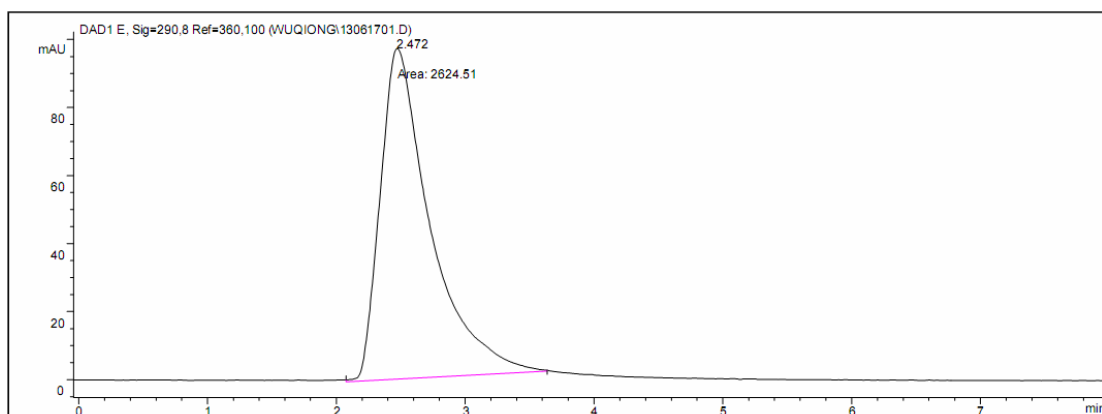


Figure S24. The HPLC analysis of complex **2c**

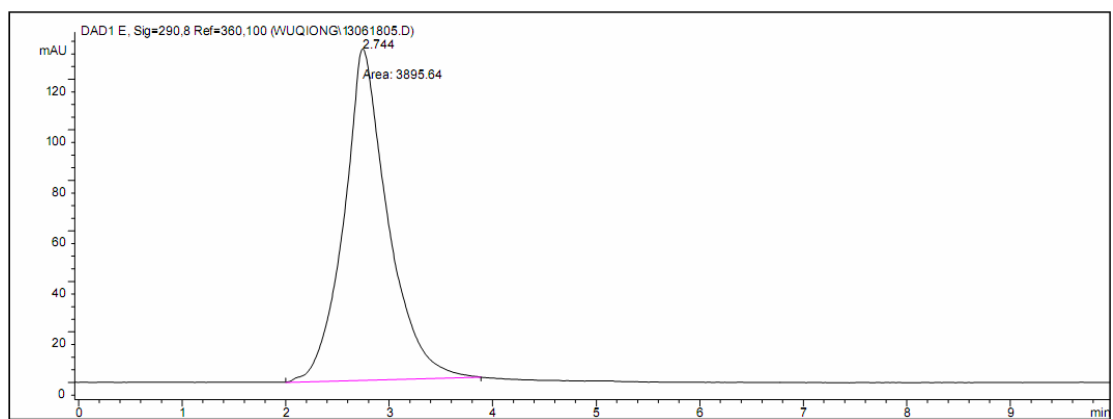


Figure S25. The HPLC analysis of complex **2d**

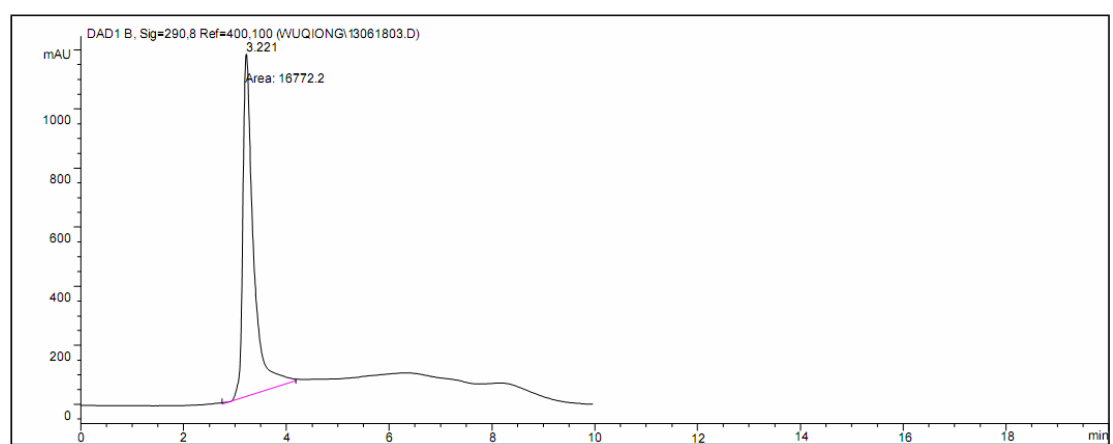


Figure S26. The HPLC analysis of complex **2e**

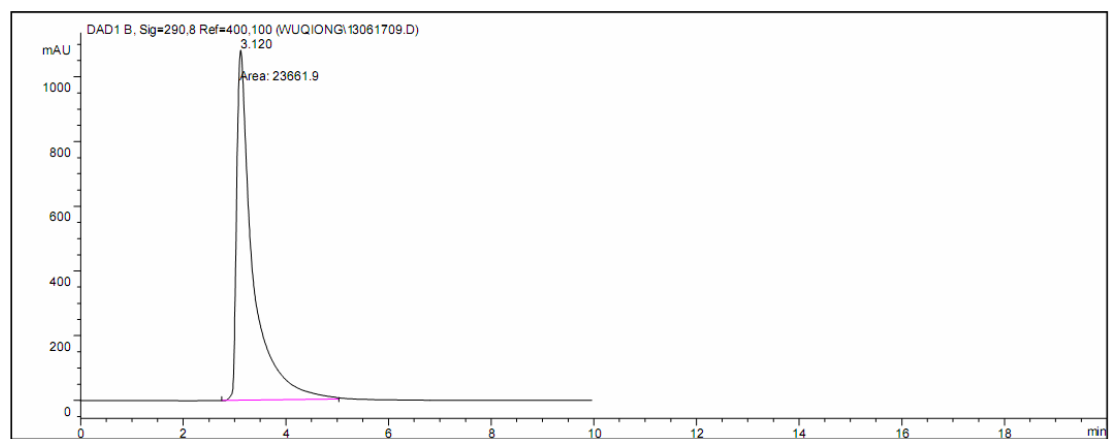


Figure S27. The HPLC analysis of complex **2f**

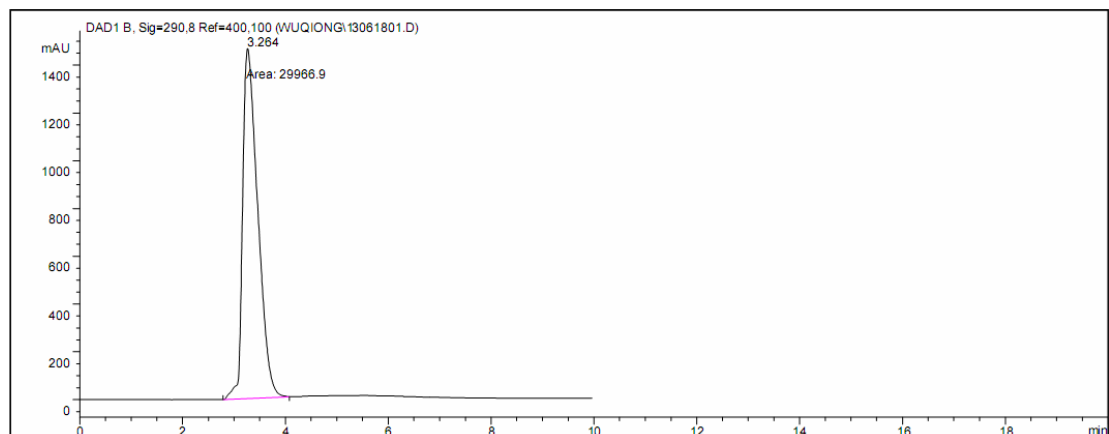


Figure S28 .The HPLC analysis of complex **2g**

### 5. The X-ray structure of complex **2e**.

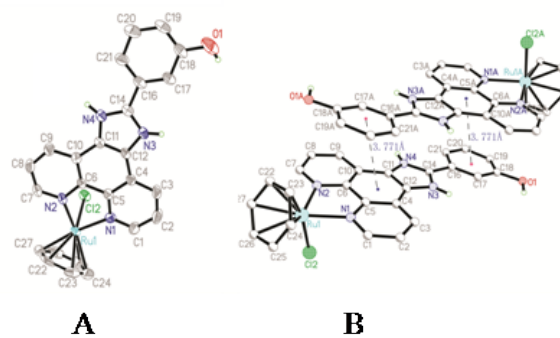


Figure S29. The ORTEP drawing of complex (**2e**) and the atom numbering in A.  $\pi$ - $\pi$  packing of the lattice for complex (**2e**) in B (CCDC NO. is 851831)

**Table S1.** Selected crystallographic data for **2e**

Identification code	<b>2e</b>
Empirical formula	C <sub>26</sub> H <sub>27</sub> Cl <sub>2</sub> N <sub>4</sub> O <sub>4</sub> Ru
Formula weight(K)	631.49
Temperature/K	293(2)
Crystal system	monoclinic
Space group	P2(1)/n
a (Å)	16.2535(11)
b (Å)	7.7798(4)
c (Å)	22.0549(14)
$\alpha$ (°)	90.00
$\beta$ (°)	107.948(4)
$\gamma$ (°)	90.00
V (Å <sup>3</sup> )	2653.1(3)
Z	8
$\rho$ calc/mg/mm <sup>3</sup>	1.581
m/mm <sup>-1</sup>	0.83
F(000)	1284
Reflections collected	3075
Independent reflections	4704[R(int) = 0.0273]
Data/restraints/parameters	4704/6/337
Goodnes-of-fit on F2	1.098
Final R indexes [I>2 $\sigma$ (I)]	R1 = 0.0592, wR2 = 0.1503
Final R indexes (all data)	R1 = 0.0768, wR2 = 0.1651
Largest idff. Peak and hole/e	1.42/-0.55



**Table S2.** Selected bond lengths (Å) and angles (°) for **2e**

Bond lengths (Å)		bond angles (°)	
Ru1-N1	2.096(5)	N2-Ru1-N1	77.35(18)
Ru1-N2	2.093(5)	N1-Ru1-C22	127.4(4)
Ru1-C22	2.159(6)	N1-Ru1-C23	100.0(3)
Ru1-C23	2.168(7)	N1-Ru1-C24	95.8(3)
Ru1-C24	2.194(7)	N1-Ru1-C25	116.3(4)
Ru1 C25	2.193(8)	N1-Ru1-C26	151.1(4)
Ru1-C26	2.185(8)	N1-Ru1-C27	166.6(4)
Ru1-C27	2.182(8)	N1-Ru1-Cl2	83.42(15)
Ru1-Cl2	2.3962(16)	N2-Ru1-C22	94.0(3)
N1-C1	1.338(8)	N2-Ru1-C23	114.1(3)
N1-C5	1.349(7)	N2-Ru1-C24	148.8(3)
N2-C6	1.355(7)	N2-Ru1-C25	166.2(4)
N2-C7	1.335(8)	N2-Ru1-C26	130.0(4)
N3-C12	1.376(7)	N2-Ru1-C27	102.2(3)
N3-C14	1.346(7)	N2-Ru1-Cl2	84.73(13)
N4-C11	1.361(7)	C22-Ru1-C23	36.9(4)
N4-C14	1.317(7)	C22-Ru1-C24	65.8(3)

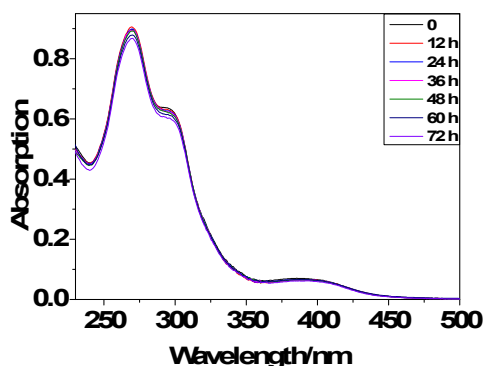


Figure S30 The UV spectra of complex **2a** (20  $\mu$ M) in water for 72 hour.

## References

1. A. Ambrus, D. Chen, J. Dai, R. A. Jones and D. Yang, *Biochemistry*, 2005, **44**, 2048-2058.
2. Z. Zhang, Q. Wang, Q. Wu, X. Y. Hu, C. X. Wang, W. J. Mei, Y. Y. Tao, W. L. Wu and W. J. Zheng, *Chem. J. Chinese Universities*, 2012, **33**, 2441-2446.
3. H. K. Liu and P. J. Sadler, *Acc. Chem. Res.*, 2011, **44**, 349-359.
4. T. Chen and Y. S. Wong, *Biomed. Pharmacother.*, 2009, **63**, 105-113.
5. T. Chen and Y. S. Wong, *J. Agric. Food Chem.*, 2008, **56**, 10574-10581.
6. X. Lu, K. Zhu, M. Zhang, H. Liu and J. Kang, *J. Biochem. Biophys. Methods*, 2002, **52**, 189-200.
7. Y. N. Gopal, D. Jayaraju and A. K. Kondapi, *Biochemistry*, 1999, **38**, 4382-4388.
8. A. A. Jain, M. R. Rajeswari, *Biochim. Biophys. Acta.* 1622 (2003) 73-81.
9. V. Brabec, V. Kleinwachter, J. L. Butour, N. P. Johnson, *Biophys. Chem.* 35 (1990) 129-141.